



## Electron spin resonance study of chemical reactions and crossover processes in a fuel cell: Effect of membrane thickness

Lu Lin, Marek Danilczuk<sup>1</sup>, Shulamith Schlick\*

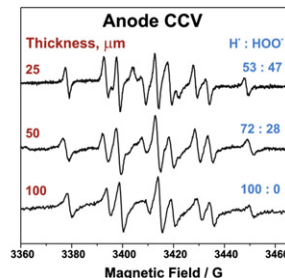
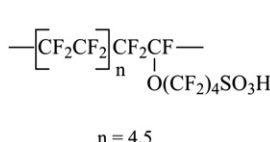
Department of Chemistry and Biochemistry, University of Detroit Mercy, 4001 W. McNichols Road, Detroit, MI 48221-3038, USA

### HIGHLIGHTS

- Spin trapping ESR experiments were performed *in situ*, in a fuel cell.
- Detection of unstable intermediates was possible with DMPO as the spin trap.
- Effect of membrane thickness on the intensity of spin adducts was determined.
- DMPO/H and DMPO/OOH adducts were detected in most experiments.

### GRAPHICAL ABSTRACT

#### 3M Membrane (EW 825)



### ARTICLE INFO

#### Article history:

Received 6 November 2012

Received in revised form

16 January 2013

Accepted 18 January 2013

Available online 29 January 2013

#### Keywords:

Electron spin resonance (ESR) spectroscopy  
Spin trapping ESR  
In-situ fuel cell  
Membrane electrode assembly (MEA)  
Gas crossover

### ABSTRACT

Spin trapping ESR experiments were performed in a fuel cell inserted in the resonator of the ESR spectrometer, and allow visualization of crossover processes and separate detection of chemical reactions at anode and cathode. The membrane-electrode assembly (MEA) consisted of the perfluorinated 3M membranes and Pt as catalyst; the detection of unstable intermediates was possible with 5,5-Dimethyl-1-pyrroline N-oxide (DMPO) as the spin trap. The major goal was to determine the effect of membrane thickness on the type and intensity of the spin adducts; MEAs with membrane thicknesses of 25 μm, 50 μm and 100 μm were studied. DMPO/H and DMPO/OOH adducts were detected in most experiments and their presence is explained by the generation of hydrogen atoms, H·, at the catalyst, and reaction with crossover O<sub>2</sub>. A strong effect of membrane thickness was detected: For a 25 μm thickness the relative intensities of DMPO/H and DMPO/OOH are similar at both anode and cathode. For 100 μm thickness the relative intensity of DMPO/H at the cathode decreased significantly, due to decreased H<sub>2</sub> crossover. At the anode DMPO/H was the *only adduct detected*; the absence of DMPO/OOH is assigned to negligible O<sub>2</sub> crossover. The results provide evidence for the involvement of hydrogen atoms in the membrane degradation. Enhancement of crossover rates in thinner membranes is expected to reduce membrane durability.

© 2013 Elsevier B.V. All rights reserved.

### 1. Introduction

Fuel cells convert the chemical energy from the reaction of H<sub>2</sub> with O<sub>2</sub> to electrical energy, and have the potential to become an alternative energy source for automotive, portable and stationary applications [1]. Proton exchange membrane fuel cells (PEMFCs) are based in many cases on perfluorinated ionomers, which consist of a perfluorinated backbone and a side chain terminated by

\* Corresponding author. Tel.: +1 313 993 1012; fax: +1 313 993 1144.

E-mail address: [schlicks@udmercy.edu](mailto:schlicks@udmercy.edu) (S. Schlick).

<sup>1</sup> On leave from the Institute of Nuclear Chemistry and Technology, Dorodna 16, 03-195 Warsaw, Poland.

sulfonic groups; their superior chemical and thermal stability, and attractive mechanical properties are important advantages [2]. Nafion is the benchmark membrane and its stability in an FC has been studied extensively. However, even Nafion can degrade under the strong oxidizing conditions in a FC [3]. Membrane degradation was assessed by a variety of characterization methods:  $^{19}\text{F}$  NMR [4], conductivity [5,6] fluoride release rate (FRR) [7–9], tensile toughness [9], and use of low-molecular-weight model compounds [10]. Additional studies have focused on the mechanism of chemical degradation due to  $\text{H}_2$  and  $\text{O}_2$  crossover [11], and oxygen reduction at the cathode in electrochemical and chemical reactions [12].

Our group has developed direct electron spin resonance (ESR) combined with DFT calculations [13–15] and spin trapping ESR studies [16,17] for the detection of short-lived oxygen radicals and membrane fragments due to degradation. Spin trapping ESR is a sensitive method for transforming short-lived intermediates into longer-lived nitroxide radicals. Use of 5,5-Dimethyl-1-pyrroline *N*-oxide (DMPO) as a spin trap, Scheme 1, allows the interpretation of the ESR spectra of the spin adducts, based on the hyperfine splittings (hfs) from  $^{14}\text{N}$  and  $\text{H}_{\beta}$  nuclei, and can lead to the identification of the trapped radicals.

Ex situ studies on model compounds have suggested that the hydroxyl radical,  $\text{HO}^{\bullet}$ , is an aggressive oxygen radical that may attack both the main- and side chains in PEMs [18]. The important role of  $\text{HO}^{\bullet}$  has been reinforced by an analysis of the stabilizing effect of Ce(III) [19]. The presence of hydrogen atoms,  $\text{H}^{\bullet}$ , has been detected for the first time in our study of Nafion fragmentation in a PEMFC inserted in the resonator of the ESR spectrometer, suggesting important mechanistic differences between ex situ experiments on model compounds and membranes, and in situ experiments in an operating FC [20]. During in situ experiments the presence of DMPO adducts were identified: the DMPO/OOH adduct was detected at the anode; and DMPO/H and DMPO/D adducts were detected at both the anode and the cathode. These studies have led to the formulation *three* degradation pathways for the PEMs: main chain unzipping, side chain attack (both by attack of hydroxyl radicals), and main chain and side chain scission by hydrogen atoms. The importance of hydrogen atoms in the in situ experiments has been demonstrated in our recent 2D spatial-spectral FTIR study; the initial step in the degradation process is abstraction of a fluorine atom from the polymer main chain and side chain by hydrogen atoms,  $\text{H}^{\bullet}$ , a step that is expected to cause both main chain and side chain scission [21]. As discussed in great detail by Coms, the reactivity of hydrogen atoms for abstraction of fluorine atoms from the C–F bonds in perfluorinated membranes is thermodynamically driven by the formation of the very strong H–F bond (136 kcal mol<sup>−1</sup>) [12]. The formation of HF was also investigated theoretically and the results have indicated that H atoms react with the C–F bond directly to form HF, and reactions with fluorine atoms bonded to secondary or tertiary carbons are most exposed to H attack [22].

Abstraction of fluorine atoms by H atoms has been verified experimentally: HF was detected by NMR in the exit stream of a fuel cell in which Nafion undergoes degradation) [4]. In our in situ ESR work, the DMPO/D adduct was detected when deuterium gas was

fed at the anode [20]. Moreover, our 2D FTIR work on fuel cell degraded Nafion MEAs has clearly shown the presence of C–H absorption bands in the IR spectrum, a result of hydrogen atoms reacting with the perfluorinated membrane [21].

The stability of perfluorinated membranes that differ in the structure of the side chain was compared in their aqueous dispersions at 300 K. The competitive kinetics (CK) approach that has been adapted for ranking the polymer stability led to the determination of their reaction rate constant with hydroxyl radicals [23]. Results have indicated an improved stability in Stabilized Nafion (in which the concentration of COOH end groups is negligible) compared to Nafion. The largest effect was, however, detected for the 3M and Aquivion polymers, which were significantly more stable. These results encouraged us to study the effect of membrane thickness in the 3M membranes, Chart 1. As seen below, the results showed that no carbon-centered radical adducts were detected in an operating FC and facilitated the interpretation of the results.

Thinner membranes are currently being used in order to reduce cost and improve fuel cells performance. As seen below, this advantage is accompanied by more extensive crossover processes that can lead to increased rates of some fragmentation processes. Thickness effects on membrane degradation have been considered [3,24] but no systematic study of the thickness effect was published. Therefore, the aim of this work was the study of chemical reactions and gas crossover processes in 3M membranes for membranes of thickness 25  $\mu\text{m}$ , 50  $\mu\text{m}$ , and 100  $\mu\text{m}$ .

## 2. Experimental section

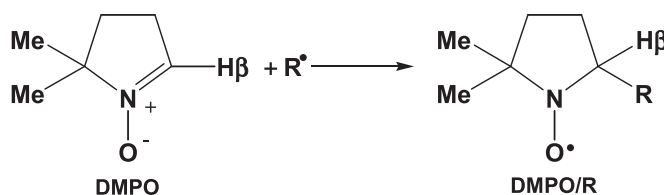
### 2.1. Materials

High purity DMPO was purchased from Enzo Life Sciences. The 3M membrane, thickness 25  $\mu\text{m}$ , was provided by 3M Company. Pt black powder with  $\geq 99.9\%$  purity was from Aldrich. Thicker membranes were prepared by pressing several layers of the thin membrane, with 3M water dispersion (18% wt) sprayed in between, at 135 °C for 10 min under a pressure of 1.5 ton/50 cm<sup>2</sup> active area [9]. The Pt ink was prepared by mixing the 3M water dispersion and Pt black powder in a ratio 1:1 w/w, dilution by deionized water, and sonication.

MEAs were prepared in our laboratory with Pt “ink” spray-cast onto the heated membrane using Master airbrush (Model G22), followed by pressing. The following steps of the MEA preparation were: placing the dry membrane on the surface of a glass plate; flattening the membrane with adhesive tape; loading the Pt ink using the airbrush; and removing the adhesive tape when the MEA is dry. The glass plate was placed on a heater during above processes and the temperature was set at 80 °C for MEA preparation. The Pt loading for all MEA samples was 0.2 mg cm<sup>−2</sup>. MEAs were prepared from 3M membranes of thickness 25  $\mu\text{m}$ , 50  $\mu\text{m}$  and 100  $\mu\text{m}$ .

### 2.2. In situ fuel cell

The FC is composed of two half-cylinders made of polystyrene cross-linked with 1,4-divinylbenzene (Rexolite), with indentation where the MEA and the electrodes were placed [20]. The FC was inserted in the resonator of the ESR spectrometer, and the temperature was controlled at 300 K. The electrodes were connected to a multimeter (HP E2377A) by platinum wires and the gas flows



**Scheme 1.** Spin Trapping by 5,5-Dimethyl-1-pyrroline-*N*-oxide (DMPO).

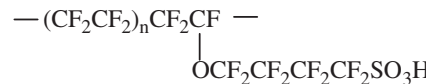


**Chart 1.** 3M membrane, EW 825,  $n = 4.5$ .

were controlled by Omega flow meters FMA2603A. The flow rates were  $2 \text{ cm}^3 \text{ min}^{-1}$  for both  $\text{H}_2$  and  $\text{O}_2$ . The dimension of the MEA was  $3 \times 18 \text{ mm}^2$ . Two types of experiments were performed, with DMPO added at the beginning of experiment (short-term), or added after 4 h of FC operation (long term). The voltage of the in situ FC was  $\approx 0.6 \text{ V}$ .

### 2.3. Spin trapping of radical intermediates

Spin-trapping ESR based on DMPO as the spin trap was used because of the spin trap selectivity for trapping oxygen-centered radicals (OCRs) and carbon-centered radicals (CCRs). In most experiments, the spin trap (approximately 1  $\mu\text{L}$  pure DMPO) was deposited either on the cathode or anode side of the MEA just before starting the FC operations. In long-term experiments, the spin trap was added after 4 h of FC operation.

### 2.4. ESR measurements

ESR spectra were recorded at 300 K using the Bruker X-band EMX spectrometer operating at 9.7 GHz and 100 kHz magnetic field modulation, and equipped with the Acquisit 32 Bit WINEPR data system version 4.33 for acquisition and manipulation, and the ER 4111 VT variable-temperature unit. The microwave frequency was measured with the Hewlett Packard 5350B microwave frequency counter. The hyperfine splittings and the relative intensities of the

spin adducts were determined by fitting the spectra using the WinSim (NIEHS/NIH) simulation package [25], with  $\approx 5\%$  margin of error. Typical acquisition parameters for the ESR spectra were: sweep width 120 G, microwave power 2 mW, time constant 20.48 ms, conversion time 41.94 ms, 2048 points, modulation amplitude 1.0 G, receiver gain  $1 \times 10^5$ , and number of scans in the range of 16–64.

## 3. Results and discussion

No ESR signals were detected for the membranes and for the corresponding MEAs in the presence or absence of gas flows; therefore all signals presented below are derived from chemical and electrochemical reactions during FC operation.

Fig. 1 shows the experimental and simulated ESR signals from in situ CCV and OCV FC operations for the 25  $\mu\text{m}$  MEA. The same adducts were detected for all operating conditions: DMPO/H and DMPO/OOH, with relative intensities  $\approx 55\%$  and  $\approx 45\%$ , respectively, and hyperfine splitting shown in Table 1.

Hydrogen atoms can be generated at the anode catalyst, reaction (1) below, leading to the presence of the DMPO/H spin adducts. The similar relative intensity of the DMPO/H at the cathode can be explained by extensive  $\text{H}_2$  crossover followed by reaction (1) at the cathode catalyst. The presence of the  $\text{HOO}^\bullet$  radical is a result of the reaction between hydrogen atoms and oxygen, reaction (2): The same relative intensity of the DMPO/OOH spin adducts at the anode

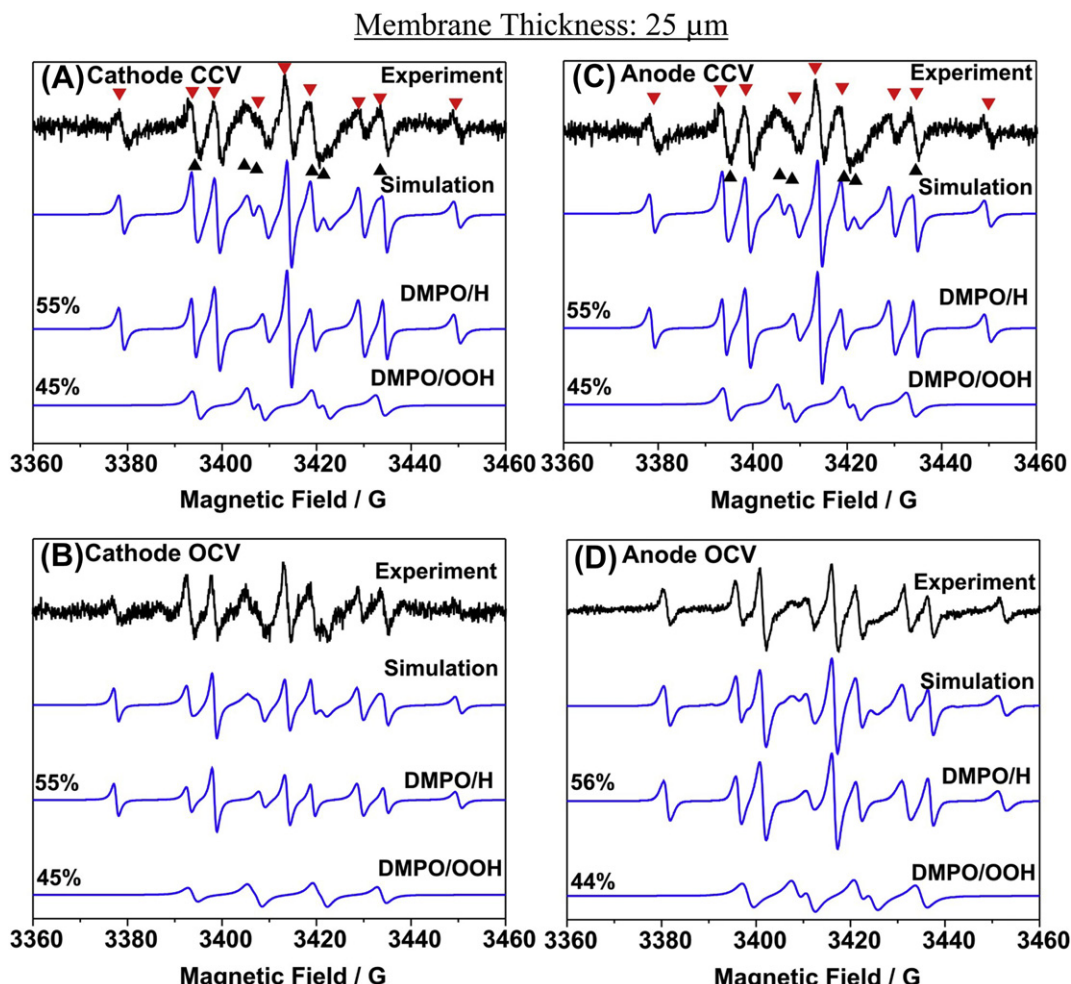


**Fig. 1.** Experimental and simulated ESR spectra of adducts when DMPO was added at the cathode side (CCV (A) and OCV (B) operations), and at the anode side (CCV (C) and OCV (D) operations). Membrane thickness: 25  $\mu\text{m}$ . In the experimental spectra 1A and 1C the signals from DMPO/H are indicated by  $\blacktriangledown$ , and for DMPO/OOH by  $\blacktriangle$ .

**Table 1**

Hyperfine splittings and relative intensities of DMPO adducts detected in the in situ fuel cell.

MEA thickness/ $\mu\text{m}$	System	Adduct	Hyperfine splittings/G		Relative intensity/%
			$a_N$	$a_H$	
25	CCV cathode (Fig. 1A)	DMPO/H	15.3	20.2 (2H)	55
		DMPO/OOH	13.7	11.5	45
	CCV anode (Fig. 1C)	DMPO/H	15.2	20.1(2H)	53
		DMPO/OOH	13.7	11.9	47
	OCV cathode (Fig. 1B)	DMPO/H	15.4	20.8(2H)	55
		DMPO/OOH	13.8	12.3	45
	OCV anode (Fig. 1D)	DMPO/H	15.2	20.3(2H)	56
		DMPO/OOH	13.2	11.3	44
50	CCV cathode (Fig. 2A)	DMPO/H	15.1	20.2(2H)	42
		DMPO/OOH	13.9	11.6	58
	CCV anode (Fig. 2C)	DMPO/H	15.2	20.2(2H)	72
		DMPO/OOH	13.3	12.1	28
	OCV cathode (Fig. 2B)	DMPO/H	15.2	20.4(2H)	46
		DMPO/OOH	13.7	11.6	54
	OCV anode (Fig. 2D)	DMPO/H	15.3	20.5(2H)	62
		DMPO/OOH	13.8	11.6	38
100	CCV cathode (Fig. 3A)	DMPO/H	15.0	19.9(2H)	25
		DMPO/OOH	13.2	12.2	75
	CCV anode (Fig. 3C)	DMPO/H	15.3	20.3(2H)	100
		DMPO/H	15.6	20.7(2H)	16
	OCV cathode (Fig. 3B)	DMPO/H	13.9	11.9	84
		DMPO/H	15.3	20.3(2H)	100

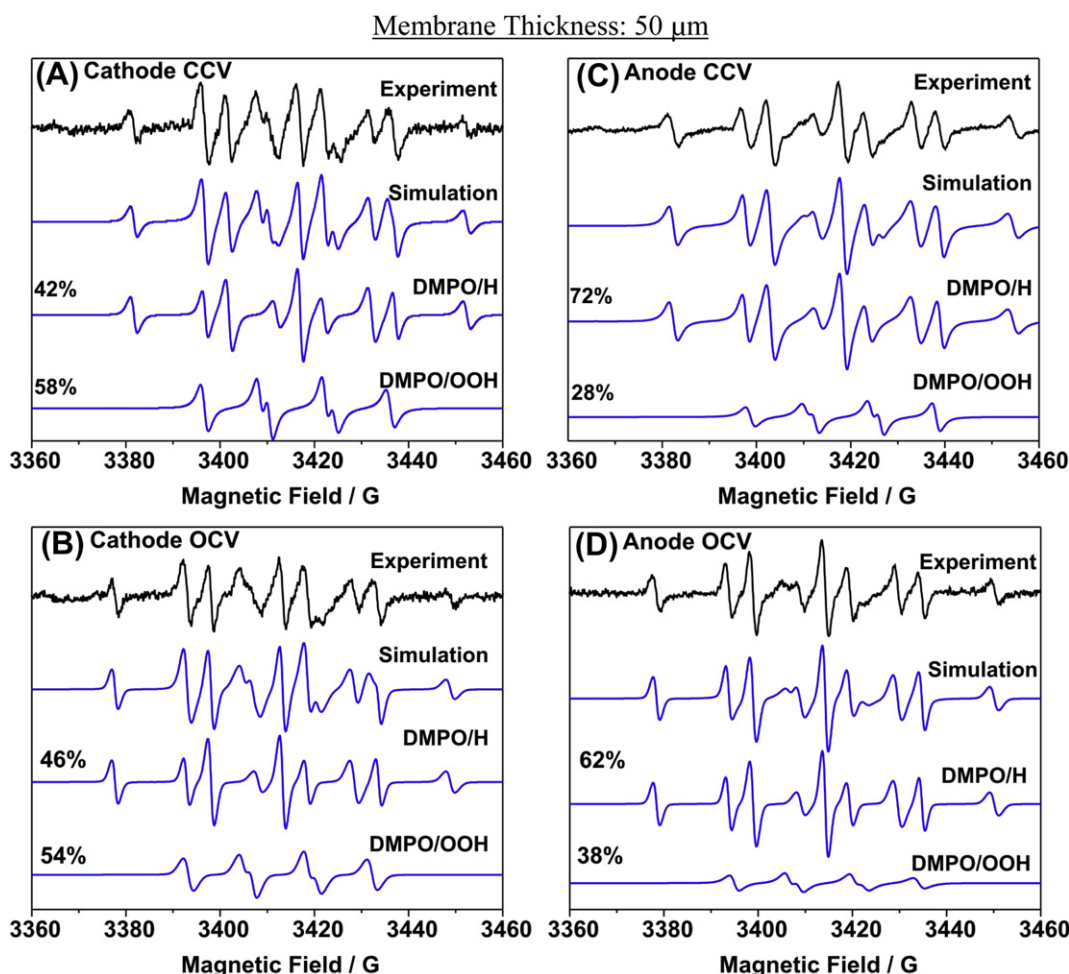


**Fig. 2.** Experimental and simulated ESR spectra of adducts when DMPO was added at the cathode side (CCV (A) and OCV (B) operations), and at the anode side (CCV (C) and OCV (D) operations). Membrane thickness: 50  $\mu\text{m}$ .

and cathode may be explained by oxygen crossover from the cathode to the anode. The results presented in Fig. 1 for the membrane of thickness 25  $\mu\text{m}$  can therefore be rationalized by  $\text{H}_2$  crossover from the anode to the cathode, and  $\text{O}_2$  crossover from the cathode to the anode.



Experimental and simulated ESR spectra for the 50  $\mu\text{m}$  MEA sample are shown in Fig. 2, for CCV and OCV FC operations. At the anode side, the relative intensity of the DMPO/H adduct increased to  $\approx 72\%$  and  $\approx 62\%$  for CCV and OCV operations, respectively. Different results were obtained at the cathode: the relative intensity of the DMPO/H adduct decreased to  $\approx 42\%$  and  $\approx 46\%$  for CCV and OCV operations, respectively. These results are clearly a result of lower  $\text{H}_2$  crossover rate from the anode to the cathode in the thicker membrane. Changes in the extent of the DMPO/H adduct are more prominent for CCV operation, possibly due to electrochemical reactions that accelerate the generation of radical species.

Experimental and simulated ESR spectra for the 100  $\mu\text{m}$  MEA sample are shown in Fig. 3, for CCV and OCV operations. A major difference was detected between the spin adducts at the cathode

and anode: both DMPO/H and DMPO/OOH were present at the cathode, while DMPO/H was the only adduct detected at the anode for both CCV and OCV operations. The absence of the DMPO/OOH adduct at the anode is indicative of negligible  $\text{O}_2$  crossover from the cathode to the anode.  $\text{H}_2$  crossover to the cathode is still possible, as seen from the presence of the DMPO/H adduct, Fig. 3A. Due to the dissolution of oxygen in water, the oxygen permeability is controlled by water diffusion and increases with water uptake and temperature. However, the water diffusivity is reduced as the membrane thickness increases [26]. The thickness effects are summarized in Fig. 4, in terms of relative intensity of the DMPO/H adduct as a function of MEA thickness.

It is interesting to note that no adducts of the hydroxyl radical ( $\text{HO}^{\cdot}$ ) or of carbon centered radicals (CCRs) were detected at the cathode side in all experiments with MEAs based on the 3M membranes, in contrast to results published for Nafion MEAs, where DMPO/OH was detected at the cathode, and DMPO/CCR was detected at the cathode and at lower intensity also at the anode [20]. The absence of the DMPO/OH adduct at the cathode and the fact that DMPO/OOH is detected at both electrodes for the 3M membranes suggest a different route for  $\text{HOO}^{\cdot}$  radicals formation compared to Nafion. Due to the high hydrogen crossover, the  $\text{H}^{\cdot}$  atoms formed at the cathode, react further with molecular oxygen to generate the  $\text{HOO}^{\cdot}$  radicals, leading to the formation of corresponding DMPO adducts.

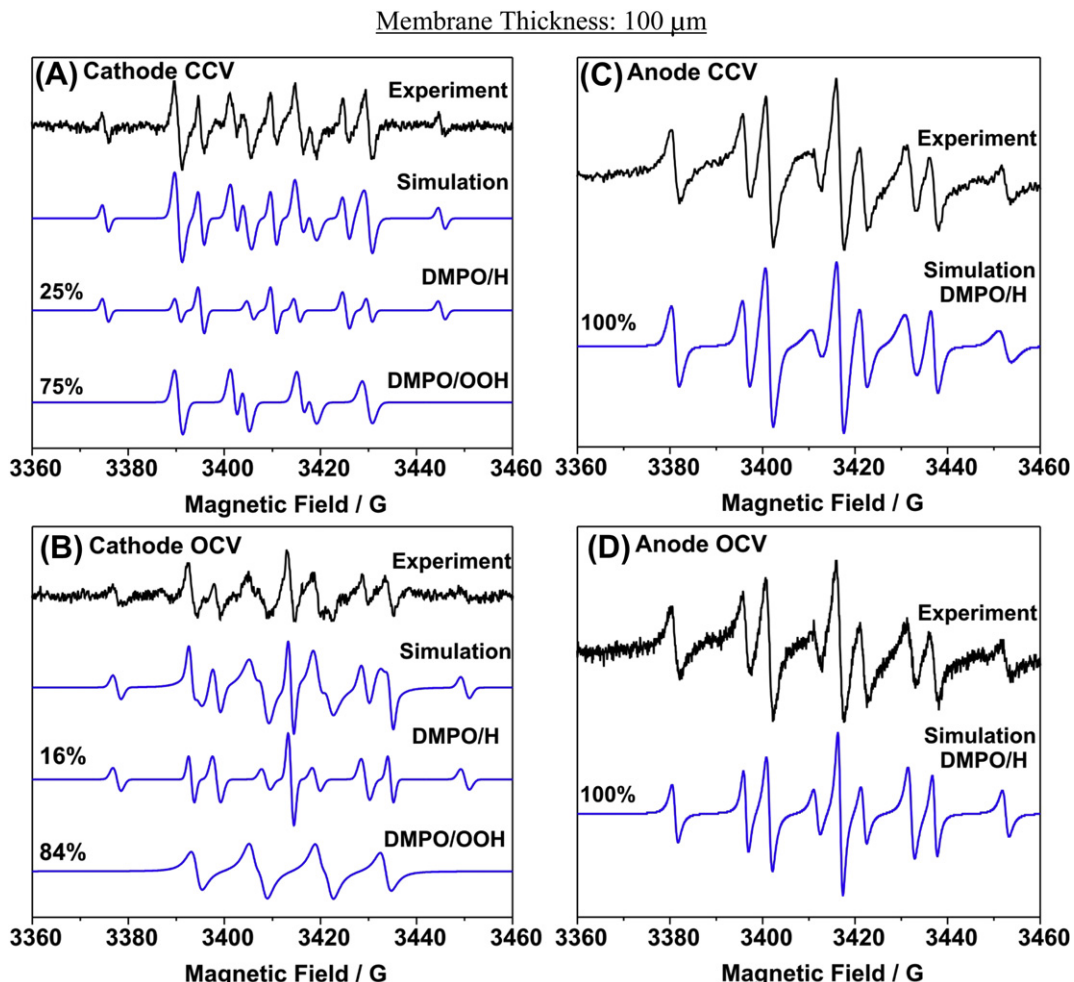


**Fig. 3.** Experimental and simulated ESR spectra of adducts when DMPO was added at the cathode side (CCV (A) and OCV (B) operations), and at the anode side (CCV (C) and OCV (D) operations). Membrane thickness: 100  $\mu\text{m}$ .

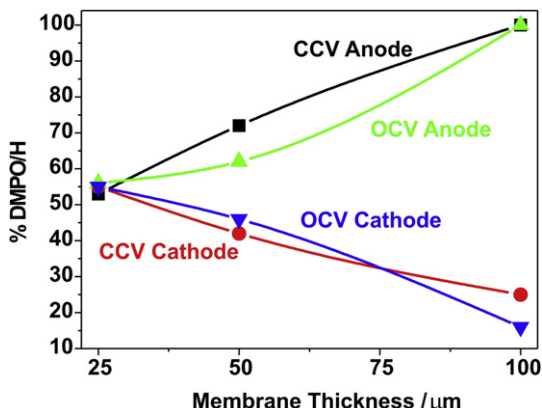


**Fig. 4.** Relative intensity of the DMPO/H adduct as a function of membrane thickness. The margin of error:  $\approx 5\%$ .

The DMPO/OH and DMPO/CCR adducts were also not detected in long-term FC experiments, an indication that the 3M membrane is more stable compared to Nafion.

#### 4. Conclusions

We have detected short-lived intermediates generated in a FC inserted in the resonator of the ESR spectrometer, as adducts of the spin trap 5,5-Dimethyl-1-pyrroline *N*-oxide (DMPO). The MEAs were based on 3M membranes with thicknesses of 25  $\mu\text{m}$ , 50  $\mu\text{m}$  and 100  $\mu\text{m}$ , and coated with Pt as catalyst.

The DMPO/H and DMPO/OOH adducts were detected at 300 K both at the cathode and anode sides for the 25  $\mu\text{m}$  and 50  $\mu\text{m}$  membranes. Hydrogen atoms can be generated at the anode catalyst, leading to the presence of DMPO/H. The presence of DMPO/H at the cathode can be explained by H<sub>2</sub> crossover followed by reaction at the cathode catalyst. The presence of the HOO<sup>•</sup> radical is a result of the reaction between hydrogen atoms and oxygen, H<sup>•</sup> + O<sub>2</sub><sup>•</sup>  $\rightarrow$  HOO<sup>•</sup>. The relative intensities of the DMPO/H adduct suggested a reduced crossover rate in the thicker membrane, 50  $\mu\text{m}$ .

Only the DMPO/H signal was observed at the anode for the 100  $\mu\text{m}$  membrane; the absence of the DMPO/OOH is compatible with negligible O<sub>2</sub> crossover. At the cathode DMPO/OOH is still present, suggesting some H<sub>2</sub> crossover even in the thickest, 100  $\mu\text{m}$ , membrane.

No adducts of the hydroxyl radical (HO<sup>•</sup>) or of carbon centered radicals (CCRs) were detected at the cathode side in all experiments with MEAs based on the 3M membranes, in contrast to results published for Nafion MEAs, where DMPO/OH was detected at the cathode, and DMPO/CCR was detected at the cathode, and at lower intensity also at the anode. The DMPO/OH and DMPO/CCR adducts

were also not detected in long-term FC experiments, an indication that the 3M membrane is more stable compared to Nafion.

#### Acknowledgments

This research was supported by the U.S. Department of Energy Cooperative agreement No. DE-FG36-07GO17006, and by the National Science Foundation (Polymers Program). DOE support does not constitute an endorsement by DOE of the views expressed in this presentation. We thank Drs. Steven Hamrock and Mark Schaberg for providing the 3M membrane of thickness 25  $\mu\text{m}$ .

#### References

- [1] M.L. Perry, T.F. Fuller, J. Electrochem. Soc. 149 (2002) S59–S67.
- [2] E. Roduner, S. Schlick, in: S. Schlick (Ed.), Advanced ESR Methods in Polymer Research, Wiley, Hoboken, NJ, 2006, pp. 197–228 (Chapter 8).
- [3] C.S. Gittleman, F.D. Coms, Y.-H. Lai, in: M. Mench (Ed.), Membrane Durability: Physical and Chemical Degradation, Elsevier, New York, 2012, pp. 15–88 (Chapter 2).
- [4] L. Ghassemzadeh, K.D. Kreuer, J. Maier, K. Muller, J. Phys. Chem. C 114 (2010) 14635–14645.
- [5] A. Pozio, R. Silva, M. De Francesco, L. Giorgi, Electrochim. Acta 48 (2003) 1543–1549.
- [6] M. Schulze, N. Wagner, T. Kaz, K.A. Friedrich, Electrochim. Acta 52 (2007) 2328–2336.
- [7] W. Liu, K. Ruth, G.J. Rusch, New Mater. Electrochem. Syst. 4 (2001) 227–231.
- [8] T. Kinumoto, M. Inaba, Y. Nakayama, K. Ogata, R. Umebayashi, A. Tasaka, Y. Iriyama, T. Abe, Z. Ogumi, J. Power Sources 158 (2006) 1222–1228.
- [9] G. Haugen, S. Barta, M. Emery, S. Hamrock, M. Yndrasaitis, in: A.M. Herring (Ed.), Fuel Cell Chemistry and Operation, American Chemical Society, Washington, DC, 2010, pp. 137–151 (Chapter 10).
- [10] D.A. Schiraldi, D. Savant, C. Zhou, ECS Trans. 33 (2010) 883–888.
- [11] M. Inaba, T. Kinumoto, M. Kiriale, R. Umebayashi, A. Tasaka, Z. Ogumi, Electrochim. Acta 51 (2006) 5746–5753.
- [12] F.D. Coms, ECS Trans. 16 (2008) 235–255.
- [13] M.K. Kadirov, A. Bosnjakovic, S. Schlick, J. Phys. Chem. B 109 (2005) 7664–7670.
- [14] A. Bosnjakovic, M.K. Kadirov, S. Schlick, Res. Chem. Intermed. 33 (2007) 677–687.
- [15] A. Lund, L. Macomber, M. Danilczuk, J. Stevens, S. Schlick, J. Phys. Chem. B 111 (2007) 9484–9491.
- [16] A. Bosnjakovic, S. Schlick, J. Phys. Chem. B 108 (2004) 4332–4337.
- [17] A. Bosnjakovic, S. Schlick, J. Phys. Chem. B 110 (2006) 10720–10728.
- [18] M. Danilczuk, F.D. Coms, S. Schlick, Fuel Cells 8 (2008) 436–452.
- [19] M. Danilczuk, S. Schlick, F.D. Coms, Macromolecules 42 (2009) 8943–8949.
- [20] M. Danilczuk, F.D. Coms, S. Schlick, J. Phys. Chem. B 113 (2009) 8031–8042.
- [21] M. Danilczuk, L. Lancucki, S. Schlick, S.J. Hamrock, G.M. Haugen, ACS Macro Lett. 1 (2012) 280–285.
- [22] T.H. Yu, Y. Sha, W.-G. Liu, B.V. Merinov, P. Shirvaniyan, W.A. Goddard, J. Am. Chem. Soc. 133 (2011) 19857–19863.
- [23] M. Danilczuk, A.J. Perkowski, S. Schlick, Macromolecules 43 (2010) 3352–3358.
- [24] X.-Z. Yuan, S. Zhang, S. Ban, C. Huang, H. Wang, V. Singara, M. Fowler, M. Schulze, A. Haug, A. Friedrich, R. Hiesgen, J. Power Sources 205 (2012) 324–334.
- [25] <http://www.niehs.nih.gov/research/resources/software/tools/index.cfm>
- [26] H.F.M. Mohamed, K. Ito, Y. Kobayashi, N. Takimoto, Y. Takeoka, A. Ohira, Polymer 49 (2008) 3091–3097.